ARTICLE
Journal of Cellular Biochemistry 114:2405–2414 (2013)

Journal of Cellular Biochemistry

Stable Expression of MutLγ in Human Cells Reveals No Specific Response to Mismatched DNA, But Distinct Recruitment to Damage Sites

Lennart M. Roesner,[1]* Christian Mielke,[2] Silke Fähnrich,[1] Yvonne Merkhoffer,[1] Kurt E.J. Dittmar,[3] Hans G. Drexler,[1] and Wilhelm G. Dirks[1]

[1]*Department of Human and Animal Cell Lines, Leibniz-Institute DSMZ-German Collection of Microorganisms and Cell Cultures, Braunschweig, D-38124, Germany*

[2]*Institute of Clinical Chemistry and Laboratory Diagnostics, Heinrich–Heine-University, Medical School, Düsseldorf, D-40225, Germany*

[3]*Helmholtz Centre of Infection Research, Braunschweig, D-38124, Germany*

ABSTRACT

The human DNA mismatch repair (MMR) gene family comprises four MutL paralogues capable of forming heterodimeric MutLα (MLH1-PMS2), MutLβ (MLH1-PMS1), and MutLγ (MLH1-MLH3) protein complexes. Human MutL subunits PMS2 and MLH3 contain an evolutionarily conserved amino acid motif DQHA(X)2E(X)4E identified as an endonucleolytic domain capable of incising a defective DNA strand. PMS2 of MutLα is generally accepted to be the sole executor of endonucleolytic activity, but since MLH3 was shown to be able to perform DNA repair at low levels in vitro, our aim was to investigate whether or not MLH3 is activated as a backup under MutLα-deficient conditions. Here, we report stable expression of GFP-tagged MLH3 in the isogenic cell lines 293 and 293T which are functional or defective for MLH1 expression, respectively. As expected, MLH3 formed dimeric complexes with endogenous and recombinant MLH1. MutLγ dimers were recruited to sites of DNA damage induced by UVA micro-irradiation as shown for MutLα. Surprisingly, splicing variant MLH3Δ7 lacking the endonucleolytic motif displayed congruent foci formation, implying that recruitment is not necessarily representing active DNA repair. As an alternative test for repair enzyme activity, we combined alkylation-directed DNA damage with comet formation assays. While recombinant MutLα led to full recovery of DNA damage response in MMR deficient cells, expression of MutLγ or single MLH3 failed to do so. These experiments show recruitment and persistence of MutLγ-heterodimers at UVA-induced DNA lesions. However, we demonstrate that in a MutLα-deficient background no DNA repair-specific function carried out by MutLγ can be detected in living cells. J. Cell. Biochem. 114: 2405–2414, 2013.

KEY WORDS: DNA MISMATCH REPAIR (MMR); MLH3; UV MICRO-IRRADIATION; DNA DAMAGE RECRUITMENT; DNA DAMAGE RESPONSE (DDR); DNA ALKYLATION DAMAGE

The DNA mismatch repair (MMR) pathway has evolved to correct errors made by DNA polymerase during DNA replication. Mutations in human MMR genes segregate with hereditary non-polyposis colorectal cancer (Lynch Syndrome), which accounts for 2–15% of total colorectal cancer cases [Lynch et al., 1997, 2009; Samowitz et al., 2001; Barnetson et al., 2006; Campbell et al., 2009]. Depending on whether a MutSα or a MutSβ failure generates the compulsory mutator phenotype, genomic instabilities arise at mono- or polymorphic DNA sequences known as microsatellite instability (MSI) serving as a diagnostic marker for defective MMR [Peltomaki, 2003; Umar et al., 2004]. The mammalian MMR gene family consists of several members homologous to either bacterial MutS or MutL which are capable to form heterodimeric complexes within the S or L subgroup (reviewed in Iyer et al., [2006]). The formation of heterodimers is shown to be a crucial step for nuclear import and is fundamental regarding damage recognition and DNA incision by mammalian MutS or MutL homolog dimers, respectively [Brieger et al., 2005]. MutS recognition of mismatched DNA base pairs resulting

The authors declare no conflict of interest.

*Correspondence to: Lennart M. Roesner, Division of Immunodermatology and Allergy Research, Department of Dermatology and Allergy, Hannover Medical School, Carl-Neuberg-Str. 1, J3 Block2, H0 2250, 30625 Hannover, Germany. E-mail: roesner.lennart@mh-hannover.de

Manuscript Received: 8 February 2013; Manuscript Accepted: 1 May 2013

Accepted manuscript online in Wiley Online Library (wileyonlinelibrary.com): 20 May 2013

DOI 10.1002/jcb.24591 • © 2013 Wiley Periodicals, Inc.

from polymerase replication errors initiates recruitment of MutL to form a ternary complex. The PMS2 subunit of MutLα was recently shown to bear a metal-binding endonuclease domain capable of generating single strand nicks in the erroneous DNA strand, which serve as a entry sites for Exonuclease I. The DNA incising activity is dependent on intactness of the $DQHA(X)_2E(X)_4E$ motif, which is found exclusively in MLH1 partners PMS2 and MLH3 and is absent in PMS1 [Kadyrov et al., 2006]. Recent data regarding resolution of holliday junctions strongly suggest this motif to be functional also in MLH3 since Exonuclease 1 is not required and a single base mutation within that site abrogates enzyme function in meiosis [Zakharyevich et al., 2010, 2012].

The multifaceted MMR system bears also functions in signal cascades towards cell cycle control and apoptosis (reviewed in Jiricny [2006]). The alkylation base damage O^6-methylguanine (O^6-meG) resulting from treatment with S_N1-methylating agents is transformed into guanine-thymidine base pair mismatches during DNA replication. Since replicative DNA polymerases are unable to insert the appropriate nucleotide opposite to O^6-meG, detection and repair by the MMR system leads to futile repair cycles and/or direct signalling to checkpoint kinases, resulting in recurrent cell cycle arrests at G2/M, formation of DNA double-strand breaks (DSBs) and finally inducing apoptosis [Karran and Marinus, 1982; Mojas et al., 2007; Quiros et al., 2010].

Human MLH3 shares the endonucleolytic domain of PMS2 and its ability to bind MLH1. This structure–function similarity gives rise to the idea of a redundant role of MLH3 in MMR, which is also well established in yeast (while PMS2 is termed PMS1 in yeast) [Flores-Rozas and Kolodner, 1998]. Further evidence was provided by reports on the association of defective MLH3 with MSI in mice [Chen et al., 2005, 2008], and its participation in MMR as shown in a human cell free-system, detecting MLH3-mediated single-strand breaks in vitro [Cannavo et al., 2005]. Multiple reports using MMR-specific knockout mice could show on one hand an essential role for MLH3 in meiotic recombination [Lipkin et al., 2002; Santucci-Darmanin et al., 2002; Kolas et al., 2005; Cohen et al., 2006], and demonstrated on the other hand the suppression of gastrointestinal and haematological tumourigenesis [Chen et al., 2005, 2008], arguing for a functional redundancy between PMS2 and MLH3 in murine MMR.

To investigate the functional role in human MMR, we stably expressed MLH3 with and without partner protein MLH1 in isogenic cells harbouring a positive and negative background of endogenous MMR. As reported previously for human MLHLα by Hong et al. [2008], we show recruitment of MutLγ complexes as a response to DNA damage by laser micro-irradiation, which has been generally acknowledged as involvement in active DNA repair processes so far. We can further demonstrate that sole expressed MLH3 and an incision-incompetent splicing variant of MLH3 also accumulated to sites of UVA-induced DNA damage. Reconstitution of MutLα function in our cells could be achieved as expected by dimeric MLH1-PMS2, triggering activation of the signalling cascade by predominant phosphorylation of CHK1/2 leading to G2/M cell cycle arrest. Unlike them, MutLγ complexes do not mediate any detectable signalling upon alkylation DNA damage. In contrast to an association of murine MLH3 with MSI, these data reveal no functional redundancy between human MutLα and MutLγ.

MATERIALS AND METHODS

PLASMID CONSTRUCTIONS

The cDNAs of human MLH1, PMS2, MLH3 and proliferating cell nuclear antigen (PCNA) were amplified by RT-PCR from primary human MRC-5 lung cells [Jacobs et al., 1970] using PCR Extender Polymerase Mix (5prime, Hamburg, Germany). The PCR primers were designed using sequence information from GenBank providing appropriate restriction sites for cloning of respective PCR products in frame with green fluorescent protein (GFP; Clontech) or TagRFP (Evrogen, Moscow, Russia) into vectors conferring bicistronic expression of two genes of interest on a single mRNA [Dirks et al., 1993]. cDNAs were fused N-terminally and in frame to GFP/TagRFP sequences and C-terminally to an internal ribosomal entry site (IRES), while latter one was fused to the selectable marker gene puromycin-*N*-acetyltransferase to be expressed in a bi- or tricistronic manner [Mielke et al., 2000].

CELL CULTURE AND GENERATION OF STABLE CELL LINES

The human fibrosarcoma cell line HT-1080 (DSMZ, Braunschweig, Germany, ACC 315) was grown in 90% Dulbecco′s MEM supplemented with 10% fetal bovine serum, 100 U/ml penicillin, 100 μg/ml streptomycin, and Glutamax-I (Invitrogen, Karlsruhe, Germany) at 37°C with 10% CO_2 Subculturing was achieved by splitting near-confluent cultures about 1:5 every 3 days using trypsin/EDTA. Human embryonal kidney cell lines 293 and 293T (DSMZ ACC 305 and ACC 635, respectively) were cultured in 90% Dulbecco′s MEM and 10% FBS at 37°C with 10% CO_2 Subculturing was achieved by splitting confluent cultures about 1:5 every 3 days by detaching cells by tapping the culture flasks. Cells were transfected with plasmid DNA using SuperFect Transfection Reagent according the manufacturer´s guideline (Qiagen, Hilden, Germany). Forty-eight hours after transfection selective pressure was applied by DMEM medium containing 0.4 μg/ml for HT-1080 and 0.7 μg/ml puromycin for 293 and 293T cells, respectively. After 14–20 days at least 10 stable transgenic clones of each transfection have been isolated, expanded and analyzed for double fluorescence and exclusive nuclear localization. At least three single clones from independent transfection experiments showing stable expression of sole recombinant MLH1, MLH3, PMS2, and PCNA or respective gene combinations thereof have been used for experiments to avoid genomic integration effects. Authenticity of single clones was confirmed by STR typing and SV40 T-antigen detection for discrimination 293 and 293T cell lines [Dirks et al., 2005].

MICROSCOPY AND FRAP EXPERIMENTS

Fluorescence images were obtained using a Zeiss LSM UV 510 Meta laser scanning microscope using laser lines of 488 and 543 nm to excite GFP and TagRFP fluorophors, respectively, in combination with a Plan-NeoFluar 40x/1.3 oil immersion objective (Zeiss, Jena, Germany). To achieve optimal conditions for live cell imaging, a heating stage in combination with an incubation unit and an active gas mixer (ibidi, Martinsried, Germany) were applied to the

microscope and were established as described above. Furthermore, an objective heater (Zeiss) guaranteed no cooling by the objective itself. Fluorescence recovery after photobleaching (FRAP) was carried out as described [Snapp et al., 2003] by bleaching a defined area inside the nucleus (11.2 μm^2) with 25% laser power, 100% transition and 20 iterations. Several images were taken before bleaching, followed by one image directly after the bleach and consecutive images every 2 s with 5% transition. Fluorescence intensity was measured at each time point. Background was subtracted before fluorescence loss due to monitor bleaching was normalized, to calculate relative intensity $I_{rel} = T_0 \times I_t/T_t \times I_0$, where T is the total cellular intensity at the time points 0 and t and I the average intensity of the bleached region at the time points 0 and t.

UVA MICRO-IRRADIATION DNA DAMAGE ASSAY

Exposure of sub-nuclear areas to defined energy doses of UVA light ($\lambda = 364$ nm) using a laser (Enterprise II, Coherent GmbH, Dieburg, Germany) focussed through the lens was done as described by Mielke et al. [2007]. Laser doses of up to 250 J/cm^2 were applied to a defined region inside the nucleus sized 5.5 $\mu m \times 550$ nm. Laser intensity was regulated by changing settings in laser power, transition, scan speed, and beam iterations.

ANTIBODIES

Detection of proteins by Western blotting was achieved by using the following antibodies: mouse αMLH1 (Oncogene Research Products, San Diego, NA28), mouse αPMS2 (NA30), mouse αMSH2 (BD Biosciences, Heidelberg, Germany, M34520), mouse αMSH3 (BD Biosciences, M94120), mouse αMSH6 (BD Biosciences, G70220), rabbit αPCNA (Abcam, Cambridge, UK, ab19167), mouse αtRFP (Evrogen, AB233), rabbit αGFP (US Biological, MA), mouse α γH2AX (Abcam, ab-22551-100, phospho-serine 139), mouse αCHK1 (Cell Signaling, #3440S), rabbit αpCHK1 (Cell Signaling, phospho-serine 345, #2348S), mouse αCHK2 (Cell Signaling, #2360S), rabbit αpCHK2 (Cell Signaling, phospho-threonine 68, #2661S). Following secondary antibodies against the species of the first antibody coupled to horseradish peroxidase were used: goat anti-mouse (Alexa 488, Invitrogen, CA), goat anti-rabbit (FITC, BIOZOL, Eching, Germany). Proteins bands became visible by use of Enhanced Chemoluminesence Kit (Perkin Elmer, Waltham).

CO-IMMUNOPRECIPITATION AND AFFINITY PURIFICATION OF MLH3 BINDING PARTNERS

For detection of endogenous binding partners, MLH3 was *N*-terminally fused to 6xHis-tag sequence by oligonucleotides and re-inserted into the corresponding bicistronic vector. Affinity purification was achieved by gravity flow columns (IBA, Göttingen, Germany) and eluate fractions were tested for binding partners by Western blotting. Co-immunoprecipitation was performed by use of the non-cross-reacting antibodies directed GFP and TagRFP and subsequent to protein G-Sepharose using Nuclear Complex Co-IP Kit (Active Motif, Rixensart, Belgium) according manufacturer´s guidelines.

IMMUNOFLUORESCENCE

For γH2AX immunodetection, cells were grown on chamber slides (Lab-Tek, Rochester, NY) and washed twice using PBS. Fixation of cells was carried out in 4% paraformaldehyde for 15 min at 37°C followed by permeabilization for 15 min using in 100 mM Tris–HCl pH 7.4, 50 mM EDTA pH 8, 0.5% Triton-X 100. Coating for blocking unspecific antibody binding was achieved over night with 3% bovine serum albumine (BSA) in PBS supplemented with 0.1% Tween20. Incubation with α-γH2AX-antibody at a dilution of 1:500 in PBS, 1% BSA, 0.1% Tween20 was carried out for 2 h at room temperature. Samples were washed three times in PBS with 1% BSA for 15 min and incubated with a respective secondary antibody diluted at 1:600 in PBS, 1% BSA, 0.1% Tween20 for 2 h at room temperature. The slides were subjected two times to final washes in PBS/1% BSA and mounted using VectaShield Mounting Medium (Vector Laboratories, Burlingame, CA).

TREATMENT OF CELLS WITH METHYLATING AGENTS

Cells were grown in tissue culture flasks at a density of 15,000 cells/cm^2. After washing with PBS, adherent cells were pre-incubated with O_6-benzylguanine (O_6BG, completely dissolved in methanol; Sigma–Aldrich, St. Louis) at a final concentration of 25 μM in DMEM/10% FBS for 2 h. Cells were treated with 50 μM temozolomide (Sigma–Aldrich, dissolved in DSMO) and 10 μM O_6BG in DMEM/10% FBS for 3 h of incubation at 37°C temperature and 10% CO_2. Cells were finally washed two times with PBS and grown for 72 h in DMEM/10% FBS and 5 μM O_6BG before subjecting to the comet assay, immunofluorescence, flow cytometry, or Western blot analysis.

ALKALINE SINGLE CELL ELECTROPHORESIS (COMET ASSAY)

Microscope slides (Menzel, Germany) were coated with 1.5% Agarose and air-dried over night. Cells were washed in PBS, warmed to 37°C and resuspended in liquid 0.5% low melting-point agarose/BSA at 2×105 cells/ml. Two 50 μl cell suspension-droplets were applied to each slide. After solidification of agarose at 4°C for 10 min, slides were covered with precooled lysis buffer (2.5 M NaCl, 100 mM EDTA, 10 mM Tris pH 10, 1% v/v Triton-X100) and incubated 30 min at 4°C. After draining the slides, incubation in precooled alkali buffer (1 mM EDTA, 300 mM NaOH) was performed at 4°C for exactly 20 min. For gelelectrophoresis, slides were placed in a suitable chamber (Horizon 11*14) and covered with 4°C alkali buffer. After applying 25 V, alkali buffer was added or removed, until a current of 300 mA was reached, and kept constant for 40 min. Slides were incubated for 5 min two times in water and once in 70% EtOH. After air-dry of the samples at 37°C, 50 μl of SYBR Green I, diluted 1:10,000 in TE buffer (1 mM EDTA, 10 mM Tris pH 7.5), was applied to each agarose-droplet and incubated in the dark for 5 min. Microscopy of slides was performed using an Axiovert 100 fluorescence microscope (Zeiss) after staining the nuclei using SYBR Green. Slides were analyzed by counting at least 50 cells per single clone tested, thereby discriminating round cells and comet shaped cells. Mean values and standard errors of the mean relative to each group were calculated.

CELL CYCLE ANALYSIS

For flow cytometry analysis, at least 100,000 cells were harvested with 3.5 mM EDTA–PBS buffer, fixed with 70% ethanol for 16 h at 4°C, treated with 20 μg/ml RNase A for 30 min, stained with 60 μg/ml propidium iodide for DNA content, and analyzed for cell cycle status with a FACSCalibur (Becton Dickinson). The cell cycle profiles were

calculated by using the cellquest and modfit lt software. Experiments were repeated at least twice.

RESULTS

STABLE EXPRESSION OF MLH3 IN ISOGENIC HUMAN CELL LINES PRO- AND DEFICIENT FOR MMR

Low endogenous expression levels as well as missing suitable antibodies are major problems in investigating human MLH3 expression and function. For these reasons, fluorescent MLH3 protein was generated by expressing a recombinant human MLH3 full length cDNA fused N-terminally to GFP and coupled via an IRES element to MLH1 or PCNA and puromycin acetyl-transferase (PAC) as a selective marker gene. Recently it was reported that C-terminal labeling impairs the functionality of MMR proteins [Brieger et al., 2012]. Resulting tricistronic expression units generate a single mRNA enabling physically coupled translation of stoichiometric amounts of the desired gene products [Dirks et al., 1993]. Single clones of the cell lines HT-1080, 293, and 293T have been analyzed for stable expression of the recombinant fusion proteins by fluorescence microscopy followed by Western blotting. Figure 1A shows recombinant expression and nuclear co-localization of biofluorescent MLH1 and MLH3 in a representative single clone of 293T cells, which do not express endogenous MLH1 due to epigenetic silencing (Fig. 1B). Long-term expression of recombinant fusion proteins neither altered the epigenetic status of transcriptionally silenced MLH1 in 293T nor did it stabilize endogenous protein levels of PMS2 (Fig. 1C). Physical interaction of GFP-MLH3 and endogenous MLH1 was confirmed by co-immunoprecipitation as shown in Figure 1D (for co-immunoprecipitation of GFP-MLH3 and recombinant MLH1 see Supplemental Fig. 1). Furthermore, we could not detect MSH2, MSH3, MSH6, and PMS2 protein in the precipitate, confirming specificity of dimerization and suggesting formation of functional recombinant MutLγ in a pro- and deficient background of otherwise isogenic 293 and 293T cells.

MUTLγ ACCUMULATES AT SITES OF UVA-MEDIATED DNA DAMAGE THROUGHOUT G1, S, AND G2

Recent publications could demonstrate the involvement of human MutS and MutL complexes in recruitment to laser-induced lesions [Hong et al., 2008].

Addressing the question whether MutLγ is also part of the repair foci, we performed live cell imaging in combination with UV-A induced DNA damage using a confocal microscope. To further investigate, if there is any cell cycle specificity for DNA repair, we stably co-expressed GFP-MLH3 together with fluorescently tagged PCNA for distinguishing G1, S and G2 phase in MMR proficient HT-1080 cells. Figure 2A indicates recombinant TagRFP-PCNA localized in DNA replication foci during S-phase, while expression of endogenous PCNA is not interfered (Fig. 2B). In contrast to PCNA, localization of MutLγ is neither immobilized at any cell cycle stage nor detectable at DNA replication foci. A fast recruitment of MutLγ and PCNA was observed after UVA irradiation, occurring at all stages of the cell cycle. Since PCNA is known to be essential and serving as a marker for DNA replication [Celis and Celis, 1985], it is noteworthy, that TagRFP-PCNA accumulated during S-phase to a lesser extent to irradiated sites (see Fig. 2A, mid and late S-phase). MutLγ was recruited to UVA-irradiated areas of the nucleus at all cell cycle stages

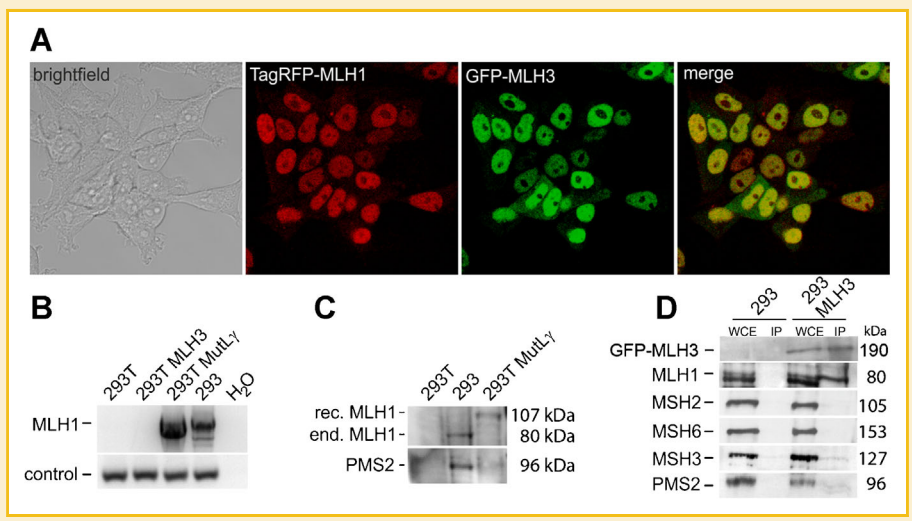

Fig. 1. Expression of dimeric MutLγ in MMR-deficient 293T cells. A: Brightfield image of recombinant 293T (left) and fluorescent images of GFP-MLH3 and TagRFP-MLH1 fusion proteins. B: RT-PCR detection of MLH1 transcripts in parental 293T, a stably transfected 293T clone expressing GFP-MLH3 and a stably transfected 293T clone co-expressing MLH1/MLH3 (MutLγ). MMR-proficient 293 cells served as a positive control for MLH1 (1,230 bp) mRNA expression. Successful reverse transcription of mRNA was confirmed by amplification of a 250 bp intron-overspanning fragment of abl kinase (control), which would otherwise generate a 740 bp genomic abl PCR fragment. C: Western blot analysis of whole cell extracts of the indicated cell lines for endogenous and recombinant MLH1 of 80 and 107 kDa, respectively, and endogenous PMS2. In contrast to 293 cell extracts (middle lane) PMS2 could not be detected in parental and recombinant 293T cell extracts. D: Co-immunoprecipitation of recombinant GFP-MLH3 in 293 cells using polyclonal αGFP antibodies and subsequent analysis of the precipitate by monoclonal αMLH1 antibodies confirmed MLH1 as endogenous partner of recombinant MLH3 (minor upper of the double band). Western blotting of equal amounts of immune precipitate using further MMR-specific antibodies generated faint bands with regard for MSH3 and PMS2, but not for MSH2 and MSH6. IP, imunoprecipitate; WCE, whole cell extract.

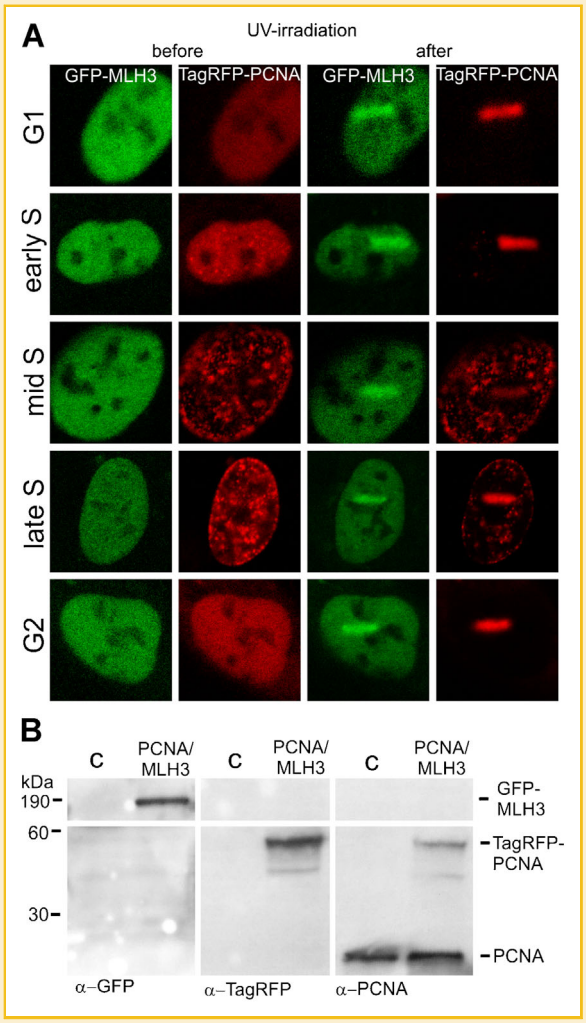

Fig. 2. Live cell imaging of GFP–MLH3 accumulation at sites of UVA–mediated DNA damage during different stages of the cell cycle. A: GFP–MLH3 and TagRFP–PCNA fusion proteins were stably generated in HT–1080 cells and images were taken before UV–irradiation at different stages of the cell cycle (left, cell cycle determination according to Celis and Celis [33]). UV–irradiation was performed using a wavelength of 364 nm. B: Western blot analysis of HT–1080 cells expressing GFP–MLH3 and TagRFP–PCNA fusion proteins. GFP–, TagRFP–, and PCNA–specific antibodies displayed absence of cross–reactivity of applied antibodies and showed no reduction of endogenous PCNA by recombinant PCNA expression. Parental HT–1080 cells served as a control (C).

in equal measure, indicating immobilization of PCNA but not of MutLγ in S-phase. PCNA is described as a loading platform and coordinator of enzyme activities in DNA damage [Mortusewicz et al., 2008], therefore recruitment and co-localization of MLH3 and PCNA suggest that MLH3, just as shown for MLH1 and MSH2 [Hong et al., 2008], may be a member of DNA repair.

SINGLE MLH3 AND AN ENDONUCLEOLYTIC–INCOMPETENT VARIANT ARE RECRUITED TO UV–A INDUCED DNA DAMAGE

Upon UVA irradiation of MLH1-deficient 293T cells, full recombinant MutLγ complexes accumulated at damaged sites (Fig. 3A). Surprisingly, solely expressed GFP-MLH3 showed a buildup with same

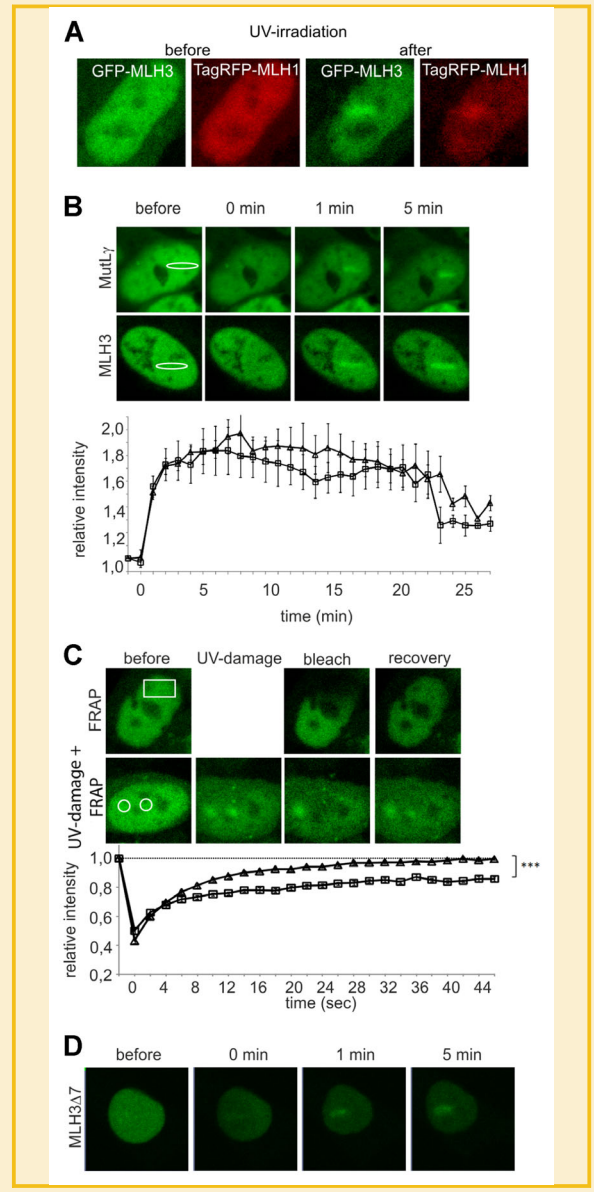

Fig. 3. Recombinant MutLγ, sole MLH3, and an incision–incompetent MLH3Δ7 variant accumulate at UVA–induced DNA damage sites. A: Recombinant Mutlγ complexes of co–expressed TagRFP–MLH1 and GFP–MLH3 in MMR–deficient 293T cells are shown before (left) and after UVA irradiation (right). Emerging green and red fluorescence clusters displayed no differences in accumulation kinetics (data not shown). B: UVA–irradiated areas of 293T nuclei harboring recombinant MutLγ or single GFP–MLH3 are indicated by white circles. Upon irradiation, images have been taken every 60 s. Resulting accumulation curves are calculated by graphs representing data of at least six independent measurements. C: Upper row: FRAP. Upon photobleaching of GFP–MLH3 molecules in a defined area of the nucleus (white rectangle in before image), recovery of fluorescence was documented immediately and 5 min after bleaching (bleach and recovery, respectively). Lower row: damage/FRAP. After UVA–irradiation–mediated DNA damage of two separate spots (white circles in before image), mobility of recruited GFP–MLH3 was measured by bleaching the right "damage" spot 5 min after irradiation. Subsequent images were taken every 2 s and accumulation curves were calculated for fluorescence recovery for a non–damaged (□) and UVA–damaged area (Δ). Error bars represent standard error of the mean. D: 293T cells stably transfected with MLH3Δ7, an incision incompetent splice variant of MLH3, were subjected to UVA–irradiation experiments as described in (A).

accumulation kinetics as shown in Figure 3B. Investigating the possibility of a functional activity of MLH3 at the damaged site, we measured dynamic exchange rates of the fluorescent protein by photobleaching as shown in Figure 3C. While re-distribution of MLH3-molecules into a bleached area was complete to 100% within 15 s in non-damaged areas of the nucleus, bleaching of a damage-induced area led to recovery of ~80% fluorescence intensity only. These data show a high dynamic exchange and transition rate of GFP-MLH3 molecules and a decreased mobility at damaged DNA sites.

To further link recruitment to repair activity, we cloned the MLH3Δ7 variant described by Lipkin et al. [2000]. MLH3Δ7 lacks the motif $DQHA(X)_2E(X)_4E$ of exon 7 by differential splicing and is predicted to be unable for any DNA incising activity. Interestingly, foci formation of MLH3 and MLH3Δ7 was indistinguishable with regard to onset and decay of irradiation-induced foci (Fig. 3B,D). As a self-evident conclusion, this finding implies that recruitment of MLH3 is independent of the presence of the incising catalytic domain.

MLH3 IS UNABLE TO TRIGGER DNA DAMAGE-INDUCED G2/M CHECKPOINT ARREST

Since DNA damage recruitment experiments in our case give no clue on repair activity, we sought to check MLH3 activity in a MMR-specific assay for DNA damage response. Temozolomide (TMZ) is an alkylating chemotherapeutic drug, which triggers the MMR dependent checkpoint arrest inducing autophagy, senescence, and apoptosis [Knizhnik et al., 2013]. Emerging O^6-meG/C are converted to O^6-meG/T mismatches during subsequent DNA replication and are detected and processed by MMR in a futile manner, resulting in a MutLα-mediated G2/M arrest and formation of DSBs [Mojas et al., 2007; Quiros et al., 2010]. In MMR proficient cell lines, the cell cycle arrest becomes visible by a comet-like shape of migrating genomic DNA in alkali single cell electrophoresis [Stojic et al., 2004]. Subjecting parental and indicated recombinant cell lines to alkylating damage, 293T cells deficient for MMR did show background levels of comets similar to untreated control cells (Fig. 4A). Reconstitution of 293T cells with recombinant MutLα (see also Supplemental Fig. 2) led to an increase of comet formation after TMZ treatment to an extent directly comparable to MMR proficient 293 cells. Five different 293T MutLα single clones from independent transfection series showed similar levels of comet formation, indicating a restored checkpoint control pathway. In contrast, MutLγ complexes could not mediate significant comet formation compared to control cells.

Opposing the model of checkpoint arrest due to futile cycling, it has been proposed that the checkpoint is activated without incising the DNA. Due to interactions between the MMR heterodimers and damage signaling kinases, it was stated that checkpoint could also be mediated by direct signaling. Therefore, we tested whether the relevant checkpoint kinases CHK1/2 were phosphorylated after treatment with alkylating agents following the cell cycle. While upon TMZ treatment of 293 cells only low levels of CHK1-phosphorylation could be shown, CHK2 is subjected to unambiguous phosphorylation at position Thr68 in parental 293 and 293T MutLα cells (Fig. 4B). On the cellular level, checkpoint arrest was confirmed by cell cycle analysis using flow cytometry (Fig. 4C). In contrast, G2/M checkpoint

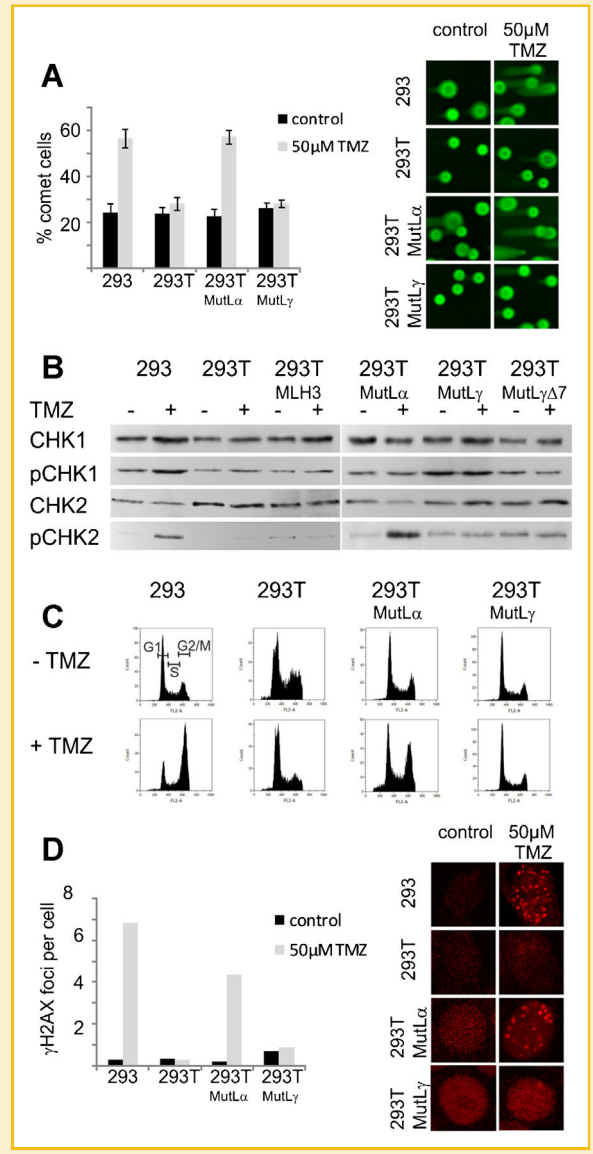

Fig. 4. TMZ-mediated activation of MMR-specific G2/M checkpoint arrest. A: Parental MMR-deficient 293T, MutLα- and MutLγ-reconstituted single clones, and MMR-proficient isogenic 293 cells were exposed to alkylating DNA damage by TMZ. Comet formation after alkali single cell electrophoresis (SCE) was used to determine the amount of arrested cells. Columns represent the mean percentage of comets of untreated cells (black bars) compared to TMZ-treated cells (gray bars). In case of reconstituted cell lines, each bar represents measurements of a minimum of seven independent single clones each with at least 50 comets analyse. Respective images of representative cells processed in SCE are shown to the right. B: Western blot analysis of parental 293, 293T, and 293T single clones transfected with indicated genes were analyzed using pairs of CHK1/-2 and their phospho-specific counterpart antibodies (pCHK1/2). C: Cell cycle analysis after treatment of indicated cell lines with 0.05 mM TMZ. Shown are representative cytometrograms of MMR proficient 293, MMR deficient 293T cells and MMR-reconstituted single clones of 293T for MutLα/γ as indicated. D: Histone H2AX phosphorylation was detected by immunofluorescence of a phosho-specific antibody. Columns represent persistent γ-H2AX damage foci in TMZ-treated cells (gray bars) and control cells (black bars). Increased levels of foci formation were quantified using ImageJ (NIH, Bethesda, Maryland). At least 50 cells were analyzed for comet formation; images to the right show representative nuclei.

arrest of 293T cells expressing MLH3 alone or paired expression with MLH1 to form dimeric MutLγ could not be observed.

The finding of the inability to signal a G2/M cell cycle arrest prompted us to analyze γH2AX foci, which are commonly used as a marker for DSBs [Rogakou et al., 1998, 1999] as well as a marker for G2/M arrested cells [Stojic et al., 2004; Quiros et al., 2010]. Figure 4D demonstrates background staining of untreated 293 and untreated recombinant 293T cell lines, while an increased quantity of γH2AX foci in 293 cells and MutLα-reconstituted 293T cells could be detected after TMZ treatment. Neither 293T cells expressing MutLγ nor 293T cells expressing MLH3 alone showed phosphorylated H2AX upon TMZ-induced DNA damage, indicating the absence of DSB formation. Thus, phosphorylation of H2AX correlates with the generation of comets, phosphorylation of CHK2 and G2/M cell cycle arrest after TMZ treatment in either 293 or 293T MutLα cells. Since comet formation and DSB generation are understood as a direct result of DNA incision by MMR [Stojic et al., 2004], these data confirm the incising capacity of human MutLα (as shown in Cejka et al. [2003]), while this holds not true for human MLH3 (Fig. 5).

DISCUSSION

In 2000, Lipkin reported on the DNA mismatch repair gene MLH3 and its association with mammalian microsatellite instability [Lipkin et al., 2000]. Further genetic studies on families bearing Lynch Syndrome have addressed the question whether or not MLH3 plays a role in MMR, but ambiguous results had generated a controversial discussion leading to different scenarios: (i) human MLH3 mutations can be found exclusively in Lynch syndrome patients with further concomitant mutations within the MMR family [Akiyama et al., 2001; Liu et al., 2003], (ii) human MLH3 deficiency does not confer any cancer-prone status [Hienonen et al., 2003; de Jong et al., 2004], and (iii) human MLH3 mutations are able to cause MSI and a mutator phenotype [Loukola et al., 2000; Wu et al., 2001].

One main problem investigating MLH3 or MutLγ in human cells is the low expression level. Competing binding partners of MLH3 as PMS1 and PMS2 are about 10–60 times more abundant, respectively, than MLH3 itself [Charbonneau et al., 2009]. Although transient expression has been reported recently [Ou et al., 2009], stable recombinant expression of wild type MLH3 and also of truncation mutants is reported to be toxic to human cell lines [Lipkin et al., 2000; Charbonneau et al., 2009]. Bypassing toxic over-expression, in vitro studies could show a slight redundancy of human MutLα and MutLγ with regard to repair of base-base mismatches [Cannavo et al., 2005], but even experiments using in-vitro translated proteins are reported to be tricky due to instability issues [Charbonneau et al., 2009]. Our results confirm reported toxicity because establishment of stably expressing clones of MLH3 was reduced by over 90% compared to control transfections (data not shown). The expression of the gene pair MLH3 and MLH1 using multistronic constructs was observed to be tolerated if quenched to a low level, indicating functional recombinant proteins with toxic potential when exceeding a specific physiologic threshold. Furthermore, biological function of MLH3 and MutLγ could be assumed by exclusive localization inside the nucleus and the ability of binding endogenous as well as recombinant partner proteins. The multicistronic expression construct offers on top of that another benefit. Since expression of the MutLγ dimer did not stabilize endogenous PMS2, which is otherwise being reported upon expression of single MLH1 in 293T cells [Cejka et al., 2003; Cannavo et al., 2007], it can be assumed that translation of multicistronic mRNAs facilitates MutLγ-dimerization due to close spatial proximity of the molecules during protein synthesis. Under these conditions, PMS2 should not interfere in experiments carried out on MutLγ with regard to endonuclease function in 293T cells. Notably, DNA damage recruitment and retained interaction with MLH1 can only indicate functionality but not assure overall intactness of the MLH3 protein, since its exact function as a whole in somatic cells is unknown.

Laser micro-irradiation systems can induce various types of DNA damage and are a sophisticated tool used to study damage response kinetics in living cells [Cejka et al., 2003]. Using a heated and CO_2-aerated stage, we recorded under physiologic conditions live cell images and specific kinetics of UVA-mediated DNA damage response of MLH3. Our recruitment data on MutLγ and MLH3 are consistent to kinetics of human MutS complexes and MLH1 as described by Hong et al. [2008], although little differences with regard to persistence and decay of accumulated fluorescence are detected, possibly due to differing energies of the used laser systems. While MSH2, MLH1 and PMS2 are able to enter the nucleus and to accumulate at sites of UVA-mediated DNA damage only as dimerized complexes [Hong et al., 2008], recruitment of sole expressed MLH3 to DNA damage sites, enabled by independent nuclear localization, is a novel finding. Photobleaching of recruited MLH3 at a damaged site led to a partial recovery of fluorescence, showing about 80% of bleached molecules being replaced by surrounding proteins and 20% remaining in place. In comparable experiments, PCNA was reported to recover up to 70% [Mortusewicz and Leonhardt, 2007], which is in the same range and

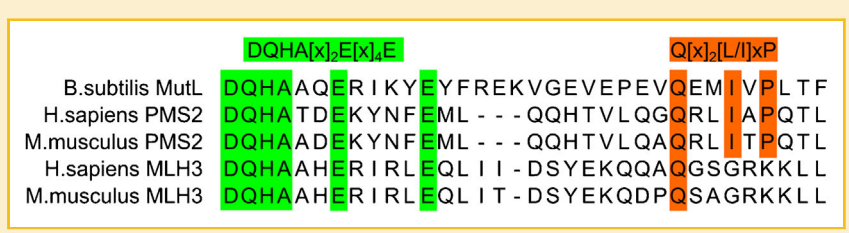

Fig. 5. Conserved putative binding motifs of MutL proteins Amino acid sequence alignment of the endonuclease motif found in MutL of Bacillus subtilis and mammalian PMS2 and MLH3 are highlighted in green. The endonuclease motif is not present in mammalian MLH1, but it is delivered by the dimerizing partners PMS2 and MLH3. The putative ß-binding motif of Bacillus subtilis MutL and the PCNA-binding motif of murine and human PMS2 and MLH3 are labeled in orange.

supports damage specificity of MLH3. In order to proof whether or not recruitment could be a marker for DNA incising activity of DNA repair, we repeated that experiment with an MLH3Δ7 isoform. This splicing variant is lacking exon 7 that carries the highly conserved endonuclease motif (Fig. 5). We detected damage-induced recruitment following equal kinetics compared to wild type MLH3, even in a MLH1-deficient background. Since the described isoform occurs naturally, we cannot exclude it to be recruited due to a regulating function. We conclude that recruitment of MutL homologues is therefore to be considered as specific for repair proteins, but does not necessarily reflect an active role in DNA repair processes.

In contrast, the ability to evoke a checkpoint arrest as a response to DNA damage arisen from treatment with SN1-alkylating agents is a distinct assay to evaluate MMR function. For MLH3, this ability has been recently investigated in knockout mice. Studies by Chen et al. [2005] showed a significant reduction in stalling the cell cycle in MEFs from $Mlh3^{-/-}$ mice and could also demonstrate an additive effect of $Mlh3^{-/-}$/$Pms2^{-/-}$ status leading to a phenotype comparable to $Mlh1^{-/-}$ mice. While this strongly argues for a function of MLH3 in MMR activity, we chose the experimental assembly of single cell electrophoresis (comet assay) as it is a frequently used method for strand break formation and damage quantification [Helma and Uhl, 2000]. Using alkylating agents, comet shape is believed to derive from multiple incisions of DNA leading to DSBs during S-phase, finally triggering ATM/ATR-mediated checkpoint arrest in which single stranded regions are sustained [Mojas et al., 2007]. A recent paper by Quiros et al. [2010] underlines the data by Stojic et al. [2004] and presents a model in which processing of TMZ-induced O^6-meG is leading to DSBs after two rounds of DNA replication, subsequently followed by apoptosis. Pre-requisition of forming DNA DSBs is the incising activity of MutLα during the futile cyclings of MMR, generating 1,000–3,000 nucleotides of single-stranded regions of DNA. The combination of TMZ-mediated DNA alkylation and the comet assay functions therefore as a test for endonucleolytic activity. Without any need for quantification of damage intensity, counting DNA spots in a true/false manner (comet/no comet) in 293T cells expressing MutLα and MutLγ gave clear evidence that no endonucleolytical activity is displayed by MutLγ. It is worth mentioning, that independent single clones of MutLα displayed all comparable intensity of fluorescence and showed comet formation indistinguishable between each other. Furthermore, our results for MutLα could confirm data from Stojic et al. [2004] with regard to comet formation, predominant CHK2 phosphorylation, G2/M cell cycle arrest and H2AX phosphorylation. Our negative results for MutLγ and also for single MLH3 and its isoform Δ7 in the comet assay exclude any functional redundancy to MutLα in the human system.

Since TMZ is generating mispairs that are detected predominantly by MutSα, we cannot exclude from our experiments that MLH3 might act only in combination with MutSβ. There are two contradictory findings concerning the target of MLH3: In order to map binding domains among in vitro-translated MMR proteins, studies by Charbonneau et al. [2009] describe specific interactions between human MLH1 and MLH3 with MSH3, suggesting exclusive interaction with the MutSβ heterodimer (MSH2–MSH3). More convincing, studies by Cannavo et al. [2005] could show that purified MutLγ from Sf9 extracts could, albeit with low efficiency, assist the correction of base-base mispairs and one-nucleotide insertion/deletion loops. These are known to be detected first of all by MutSα, just as the mispairs created in our experiment using S_N1-alkylating agents. Since Cannavo et al. further state, that the repair activity could not be detected using MutLγ at physiological concentrations, our findings are not in contrast to their work.

Our data on recruitment of MutLγ to sites of oxidized DNA damages gives rise to the idea that MLH3 is incapable of incising the mismatched DNA strand due to a negative regulation. With regard to recent publications, we favor a model of inappropriate licensing of human MLH3 for DNA incision. An earlier report [Pillon et al., 2010] showed in *B. subtilis*, that binding of the β-clamp –the bacterial homologue to human PCNA– leads to a conformational change of MutL, enabling the endonucleolytic incision. The $Q(X)_2(L/I)XP$ PCNA binding motif is highly conserved and can be found in MutLα, while only incomplete in MutLγ (Fig. 5). In contrast to *B. subtilis*, the mammalian binding motif for PCNA interaction, the so-called PIP-box is localized at MutS homologs MSH6 and MSH3 [Kleczkowska et al., 2001]. The recent publication on the crystal structure of the β-clamp [Pillon et al., 2011] revealed a PIP-box which could carry out a crucial positioning command for a proper conformation and orientation of the domain of PMS2 and licensing incision of DNA. To fulfill the putative function of resolving double Holliday Junctions during meiosis, MutLγ is believed to be licensed by other proteins, that is, Exonuclease I [Zakharyevich et al., 2010, 2012]. Following this model, MLH3 is recruited to sites of damaged DNA as shown for human MutS and MutL complexes, but is not licensed for endonucleolytic incision of the defective strand. Further studies using MLH1 and MLH3 chimera would be able to further characterize a spacial- and temporal-specific endonucleolytic activity of human MutLα and MutLγ.

REFERENCES

Akiyama Y, Nagasaki H, Nakajima T, Sakai H, Nomizu T, Yuasa Y. 2001. Infrequent frameshift mutations in the simple repeat sequences of hMLH3 in hereditary nonpolyposis colorectal cancers. Jpn J Clin Oncol 31:61–64.

Barnetson RA, Tenesa A, Farrington SM, Nicholl ID, Cetnarskyj R, Porteous ME, Campbell H, Dunlop MG. 2006. Identification and survival of carriers of mutations in DNA mismatch-repair genes in colon cancer. N Engl J Med 354: 2751–2763.

Brieger A, Plotz G, Raedle J, Weber N, Baum W, Caspary WF, Zeuzem S, Trojan J. 2005. Characterization of the nuclear import of human MutLalpha. Mol Carcinog 43:51–58.

Brieger A, Plotz G, Hinrichsen I, Passmann S, Adam R, Zeuzem S. 2012. C-terminal fluorescent labeling impairs functionality of DNA mismatch repair proteins. PLoS ONE 7:e31863.

Campbell PT, Curtin K, Ulrich CM, Samowitz WS, Bigler J, Velicer CM, Caan B, Potter JD, Slattery ML. 2009. Mismatch repair polymorphisms and risk of colon cancer, tumour microsatellite instability and interactions with lifestyle factors. Gut 58:661–667.

Cannavo E, Marra G, Sabates-Bellver J, Menigatti M, Lipkin SM, Fischer F, Cejka P, Jiricny J. 2005. Expression of the MutL homologue hMLH3 in human cells and its role in DNA mismatch repair. Cancer Res 65:10759–10766.

Cannavo E, Gerrits B, Marra G, Schlapbach R, Jiricny J. 2007. Characterization of the interactome of the human MutL homologues MLH1, PMS1, and PMS2. J Biol Chem 282:2976–2986.

Cejka P, Stojic L, Mojas N, Russell AM, Heinimann K, Cannavo E, di Pietro M, Marra G, Jiricny J. 2003. Methylation-induced G(2)/M arrest requires a full complement of the mismatch repair protein hMLH1. EMBO J 22:2245–2254.

Celis JE, Celis A. 1985. Cell cycle-dependent variations in the distribution of the nuclear protein cyclin proliferating cell nuclear antigen in cultured cells: Subdivision of S phase. Proc Natl Acad Sci USA 82:3262–3266.

Charbonneau N, Amunugama R, Schmutte C, Yoder K, Fishel R. 2009. Evidence that hMLH3 functions primarily in meiosis and in hMSH2-hMSH3 mismatch repair. Cancer Biol Ther 8:1411–1420.

Chen PC, Dudley S, Hagen W, Dizon D, Paxton L, Reichow D, Yoon SR, Yang K, Arnheim N, Liskay RM, Lipkin SM. 2005. Contributions by MutL homologues Mlh3 and Pms2 to DNA mismatch repair and tumor suppression in the mouse. Cancer Res 65:8662–8670.

Chen PC, Kuraguchi M, Velasquez J, Wang Y, Yang K, Edwards R, Gillen D, Edelmann W, Kucherlapati R, Lipkin SM. 2008. Novel roles for MLH3 deficiency and TLE6-like amplification in DNA mismatch repair-deficient gastrointestinal tumorigenesis and progression. PLoS Genet 4:e1000092.

Cohen PE, Pollack SE, Pollard JW. 2006. Genetic analysis of chromosome pairing, recombination, and cell cycle control during first meiotic prophase in mammals. Endocr Rev 27:398–426.

de Jong MM, Hofstra RM, Kooi KA, Westra JL, Berends MJ, Wu Y, Hollema H, van der Sluis T, van der Graaf WT, de Vries EG, Schaapveld M, Sijmons RH, te Meerman GJ, Kleibeuker JH. 2004. No association between two MLH3 variants (S845G and P844L) and colorectal cancer risk. Cancer Genet Cytogenet 152: 70–71.

Dirks W, Wirth M, Hauser H. 1993. Dicistronic transcription units for gene expression in mammalian cells. Gene 128:247–249.

Dirks WG, Faehnrich S, Estella IA, Drexler HG. 2005. Short tandem repeat DNA typing provides an international reference standard for authentication of human cell lines. ALTEX 22:103–109.

Flores-Rozas H, Kolodner RD. 1998. The Saccharomyces cerevisiae MLH3 gene functions in MSH3-dependent suppression of frameshift mutations. Proc Natl Acad Sci USA 95:12404–12409.

Helma C, Uhl M. 2000. A public domain image-analysis program for the single-cell gel-electrophoresis (comet) assay. Mutat Res 466:9–15.

Hienonen T, Laiho P, Salovaara R, Mecklin JP, Jarvinen H, Sistonen P, Peltomaki P, Lehtonen R, Nupponen NN, Launonen V, Karhu A, Aaltonen LA. 2003. Little evidence for involvement of MLH3 in colorectal cancer predisposition. Int J Cancer 106:292–296.

Hong Z, Jiang J, Hashiguchi K, Hoshi M, Lan L, Yasui A. 2008. Recruitment of mismatch repair proteins to the site of DNA damage in human cells. J Cell Sci 121:3146–3154.

Iyer RR, Pluciennik A, Burdett V, Modrich PL. 2006. DNA mismatch repair: Functions and mechanisms. Chem Rev 106:302–323.

Jacobs JP, Jones CM, Baille JP. 1970. Characteristics of a human diploid cell designated MRC-5. Nature 227:168–170.

Jiricny J. 2006. The multifaceted mismatch-repair system. Nature reviews. Mol Cell Biol 7:335–346.

Kadyrov FA, Dzantiev L, Constantin N, Modrich P. 2006. Endonucleolytic function of MutLalpha in human mismatch repair. Cell 126:297–308.

Karran P, Marinus MG. 1982. Mismatch correction at O6-methylguanine residues in *E. coli* DNA. Nature 296:868–869.

Kleczkowska HE, Marra G, Lettieri T, Jiricny J. 2001. hMSH3 and hMSH6 interact with PCNA and colocalize with it to replication foci. Genes Dev 15:724–736.

Knizhnik AV, Roos WP, Nikolova T, Quiros S, Tomaszowski KH, Christmann M, Kaina B. 2013. Survival and death strategies in glioma cells: Autophagy, senescence and apoptosis triggered by a single type of temozolomide-induced DNA damage. PLoS ONE 8:e55665.

Kolas NK, Svetlanov A, Lenzi ML, Macaluso FP, Lipkin SM, Liskay RM, Greally J, Edelmann W, Cohen PE. 2005. Localization of MMR proteins on meiotic chromosomes in mice indicates distinct functions during prophase I. J Cell Biol 171:447–458.

Lipkin SM, Wang V, Jacoby R, Banerjee-Basu S, Baxevanis AD, Lynch HT, Elliott RM, Collins FS. 2000. MLH3: A DNA mismatch repair gene associated with mammalian microsatellite instability. Nat Genet 24:27–35.

Lipkin SM, Moens PB, Wang V, Lenzi M, Shanmugarajah D, Gilgeous A, Thomas J, Cheng J, Touchman JW, Green ED, Schwartzberg P, Collins FS, Cohen PE. 2002. Meiotic arrest and aneuploidy in MLH3-deficient mice. Nat Genet 31:385–390.

Liu HX, Zhou XL, Liu T, Werelius B, Lindmark G, Dahl N, Lindblom A. 2003. The role of hMLH3 in familial colorectal cancer. Cancer Res 63:1894–1899.

Loukola A, Vilkki S, Singh J, Launonen V, Aaltonen LA. 2000. Germline and somatic mutation analysis of MLH3 in MSI-positive colorectal cancer. Am J Pathol 157:347–352.

Lynch HT, Smyrk T, Lynch J. 1997. An update of HNPCC (Lynch syndrome). Cancer Genet Cytogenet 93:84–99.

Lynch HT, Lynch JF, Attard TA. 2009. Diagnosis and management of hereditary colorectal cancer syndromes: Lynch syndrome as a model. CMAJ 181:273–280.

Mielke C, Tummler M, Schubeler D, von Hoegen I, Hauser H. 2000. Stabilized, long-term expression of heterodimeric proteins from tricistronic mRNA. Gene 254:1–8.

Mielke C, Kalfalah FM, Christensen MO, Boege F. 2007. Rapid and prolonged stalling of human DNA topoisomerase I in UVA-irradiated genomic areas. DNA Repair 6:1757–1763.

Mojas N, Lopes M, Jiricny J. 2007. Mismatch repair-dependent processing of methylation damage gives rise to persistent single-stranded gaps in newly replicated DNA. Genes Dev 21:3342–3355.

Mortusewicz O, Leonhardt H. 2007. XRCC1 and PCNA are loading platforms with distinct kinetic properties and different capacities to respond to multiple DNA lesions. BMC Mol Biol 8:81.

Mortusewicz O, Leonhardt H, Cardoso MC. 2008. Spatiotemporal dynamics of regulatory protein recruitment at DNA damage sites. J Cell Biochem 104:1562–1569.

Ou J, Rasmussen M, Westers H, Andersen SD, Jager PO, Kooi KA, Niessen RC, Eggen BJ, Nielsen FC, Kleibeuker JH, Sijmons RH, Rasmussen LJ, Hofstra RM. 2009. Biochemical characterization of MLH3 missense mutations does not reveal an apparent role of MLH3 in Lynch syndrome. Genes Chromosomes Cancer 48:340–350.

Peltomaki P. 2003. Role of DNA mismatch repair defects in the pathogenesis of human cancer. J Clin Oncol 21:1174–1179.

Pillon MC, Lorenowicz JJ, Uckelmann M, Klocko AD, Mitchell RR, Chung YS, Modrich P, Walker GC, Simmons LA, Friedhoff P, Guarne A. 2010. Structure of the endonuclease domain of MutL: Unlicensed to cut. Mol Cell 39:145–151.

Pillon MC, Miller JH, Guarne A. 2011. The endonuclease domain of MutL interacts with the beta sliding clamp. DNA Repair 10:87–93.

Quiros S, Roos WP, Kaina B. 2010. Processing of O6-methylguanine into DNA double-strand breaks requires two rounds of replication whereas apoptosis is also induced in subsequent cell cycles. Cell Cycle 9:168–178.

Rogakou EP, Pilch DR, Orr AH, Ivanova VS, Bonner WM. 1998. DNA double-stranded breaks induce histone H2AX phosphorylation on serine 139. J Biol Chem 273:5858–5868.

Rogakou EP, Boon C, Redon C, Bonner WM. 1999. Megabase chromatin domains involved in DNA double-strand breaks in vivo. J Cell Biol 146: 905–916.

Samowitz WS, Curtin K, Lin HH, Robertson MA, Schaffer D, Nichols M, Gruenthal K, Leppert MF, Slattery ML. 2001. The colon cancer burden of genetically defined hereditary nonpolyposis colon cancer. Gastroenterology 121:830–838.

Santucci-Darmanin S, Neyton S, Lespinasse F, Saunieres A, Gaudray P, Paquis-Flucklinger V. 2002. The DNA mismatch-repair MLH3 protein interacts

with MSH4 in meiotic cells, supporting a role for this MutL homolog in mammalian meiotic recombination. Hum Mol Genet 11:1697–1706.

Snapp EL, Altan N, Lippincott-Schwartz J. 2003. Measuring protein mobility by photobleaching GFP chimeras in living cells. Curr Protoc Cell Biol 19:21.1.1–21.1.24.

Stojic L, Mojas N, Cejka P, Di Pietro M, Ferrari S, Marra G, Jiricny J. 2004. Mismatch repair-dependent G2 checkpoint induced by low doses of SN1 type methylating agents requires the ATR kinase. Genes Dev 18:1331–1344.

Umar A, Boland CR, Terdiman JP, Syngal S, de la Chapelle A, Ruschoff J, Fishel R, Lindor NM, Burgart LJ, Hamelin R, Hamilton SR, Hiatt RA, Jass J, Lindblom A, Lynch HT, Peltomaki P, Ramsey SD, Rodriguez-Bigas MA, Vasen HF, Hawk ET, Barrett JC, Freedman AN, Srivastava S. 2004. Revised Bethesda Guidelines for hereditary nonpolyposis colorectal cancer (Lynch syndrome) and microsatellite instability. J Natl Cancer Inst 96:261–268.

Wu Y, Berends MJ, Sijmons RH, Mensink RG, Verlind E, Kooi KA, van der Sluis T, Kempinga C, van dDer Zee AG, Hollema H, Buys CH, Kleibeuker JH, Hofstra RM. 2001. A role for MLH3 in hereditary nonpolyposis colorectal cancer. Nat Genet 29:137–138.

Zakharyevich K, Ma Y, Tang S, Hwang PY, Boiteux S, Hunter N. 2010. Temporally and biochemically distinct activities of Exo1 during meiosis: Double-strand break resection and resolution of double Holliday junctions. Mol Cell 40:1001–1015.

Zakharyevich K, Tang S, Ma Y, Hunter N. 2012. Delineation of joint molecule resolution pathways in meiosis identifies a crossover-specific resolvase. Cell 149:334–347.

SUPPORTING INFORMATION

Additional supporting information may be found in the online version of this article at the publisher's web-site.

Fig. S1. Co-immunoprecipitation of recombinant MLH3 and MLH1. Whole cell extract (WCE) and co-immunoprecipitates from GFP and TagRFP antibodies (IP αGFP and IP αTagRFP, respectively) of a GFP-MLH3 and TagRFP-MLH1 co-expressing 293T single clone were submitted to Western blotting using antibodies as indicated on the right.

Fig. S2. Reconstitution of 293T with MutLα. Recombinant MutLα complexes of co-expressed mCherry-MLH1 and GFP-PMS2 in MMR-deficient 293T cells are shown before (left) and after UVA irradiation (right).